LAWRENCE
LIVERMORE
NATIONAL
LABORATORY

UCRL-PROC-220749

Structures in Molecular Clouds: Modeling

J. O. Kane, A. Mizuta, M. W. Pound, B. A. Remington, D. D. Ryutov

April 20, 2006

High Energy Density Laboratory Astrophysics
Houston, TX, United States
March 11, 2006 through March 14, 2006

Updated October 14, 2003

For submittal to Proceedings of HEDLA 2006

Structures in Molecular Clouds: Modeling

J.O. Kane[1], A. Mizuta[2], M.W. Pound[3], B.A. Remington[1], D.D. Ryutov[1]

[1]*Lawrence Livermore National Laboratory, Livermore, CA 94551, USA*
[2] *Max-Planck-Institute für Astrophysik*, Garching, Germany
[3]*Astronomy Department, University of Maryland, College Park, MD 20742, USA*

Abstract. *We attempt to predict the observed morphology, column density and velocity gradient of Pillar II of the Eagle Nebula, using Rayleigh Taylor (RT) models in which growth is seeded by an initial perturbation in density or in shape of the illuminated surface, and cometary models in which structure is arises from a initially spherical cloud with a dense core. Attempting to mitigate suppression of RT growth by recombination, we use a large cylindrical model volume containing the illuminating source and the self-consistently evolving ablated outflow and the photon flux field, and use initial clouds with finite lateral extent. An RT model shows no growth, while a cometary model appears to be more successful at reproducing observations.*

1. Introduction

The Eagle Nebula (M16) is a molecular hydrogen cloud irradiated by ultraviolet (UV) stars. It displays varied and evolving structure, including 'EGGS' and 'Pillars' [{Hester}, {Pound1998},{Castle}], and appears to have an outflow of ionized hydrogen [{Hester},{Pound}]. Our ongoing investigation of the formation of such structures [{Kane2004},{Ryutov2004},{Mizuta2005},{Mizuta2006}] involves a combination of theory and modeling. Theory and modeling of molecular cloud structures has a long history [{Kahn}, {Vandervoort}, {Axford}, {Spitzer}, {Frieman}, {BertoldiMcKee}, {LeflochLazareff}, {Williams2001}, {Sysoev}]. It is sometimes tacitly assumed that Pillar structures are simply pre-existing, and revealed through 'sculpting' of the surrounding medium by the illuminating radiation [{Hester}]. However, the Pillars of the Eagle Nebula exhibit large velocity gradients, suggesting dynamic genesis. In the present work, we attempt to predict the observed morphology, column density and velocity gradient of Pillar II of the Eagle Nebula, using dynamic models in which we illuminate two types of finite-sized initial clouds with radiating sources. The clouds are intended to produce either Rayleigh Taylor (RT) growth of an initial density or surface perturbation on a disk-shaped cloud oriented normal to the illumination, or a cometary structure [{Osterbrock},{O'DellHandron},{Capriotti},{LeflochLazareff}] arising from an initially spherical cloud. We compare the morphology of the model Pillar to the observed morphology [{Hester}], and compare the model column density and projected velocity to the observed quantities [{Pound1998}]. Recently, Williams [{Williams2001}] has investigated several dynamic scenarios for the formation of the Pillars, using initial clouds of infinite thickness, so that acceleration does not occur, and did not investigate cometary models. Cometary models have been widely investigated

[{Capriotti},{Bertoldi},{BertoldiMcKee },{LeflochLazareff}], however, not in attempts to reproduce quantitative observations of M16.

Ultimately cometary models appear to prevail. However, in our early attempts using cylindrical geometry and a very simple energy deposition model, without recombination, RT models appear superior to cometary models. Recombination suppresses linear regime RT growth, as originally shown by Kahn and Axford [{Kahn},{Axford}], and more recently confirmed [{Mizuta2005},{Mizuta2006}] with simulations in Cartesian geometry with parallel rays incident at a boundary, with recombination and associated cooling added [{Neufeld},{Williams2001}]. With very high amplitude initial 'perturbations', small comet-like structures appear at late times [{Mizuta2006}], probably resulting from nonlinear processes such as shadowing. The consistent failure of RT models to produce massive structures like the Pillars may suggest a role for the pre-existing clumpy, filamentary structure typical of molecular clouds. Formation of some smaller structure may be due to effects of the directionality of the UV radiation — the tilted radiation instability, [{Ryutov2004}], and general effects of shadowing and confinement by ablation pressure.

In the style of protostellar disk modeling by Richling, Yorke and Kaisig [{RichlingYorke}], we use a large cylindrical model volume containing a radiating point source, the evolving cloud, and the outflow. In the RT models, we use initial clouds of finite lateral extent; this allows outflow to diverge, potentially mitigating the suppression of RT by recombination. We find that RT models still show no growth, although the entire cloud may slowly evolve into a large comet. In contrast, a cometary model featuring a dense initial nucleus predicts the observed morphology, column density and velocity gradient of Pillar II, and also predicts a long, low-density extension to the tail, which may correspond to wisps in visual images [{Castle}]. The comet of Lefloch and Lazareff [{LeflochLazareff}], resulting from an initial cloud of constant density, moves many times its final length while the structure grows. In contrast, in the present model, the dense nucleus holds the tip back, reproducing the observation that the length of Pillar II is similar to its distance from the illuminating stars.

2. Models and method of analysis

In all of the models discussed here, we assume an initially motionless cloud in pressure equilibrium with itself and with a surrounding low-density medium. The illuminating source is assumed to turn on at time zero, and generally remains at constant intensity or flux, except where the central intensity or flux is briefly lowered to induce a seed perturbation (discussed below).

In our earliest modeling we attempted to reproduce observations of the Pillars. We constructed a hydrodynamics code with two-dimensional r-z cylindrical geometry, a moving orthogonal grid with variable zone size in each dimension, and Van Leer-style advection [{Kane2001},{vanLeer},{ZEUS}] modified to remedy the possibility of negative densities. We used simplistic ray tracing along the columns of the grid, and simple models for opacity and absorption. In the simple ray-tracing model, parallel planar rays originate at an x boundary of the grid are propagated in the positive x-direction toward the cloud along the 'columns' of the grid. Within one zone, attenuation of the ray intensity I and deposition of internal energy u by the ray are: $\Delta I = I \exp(-\kappa \Delta x)$ and $\Delta u = \Delta I/\Delta x \, \Delta t/r$, where ρ and k are

the mass density and opacity, respectively, of the zone, t is time, Δt is the time step, and Δx is the (variable) width of the zone in the x direction. The simple opacity model is intended to produce two conditions: 1) the evaporated material has low opacity, and 2) the cloud absorbs energy in a thin surface layer. The opacity model is: $\kappa = f(T)\ (n/n_0)\ \kappa_0$, where T is temperature, $f(T)$ =1 for $T < T_0$ and exp $\{[(T-T_0)/(A_T T_0)^2]\}$ for $T \geq T_0$. Typical values for the constants in this opacity model are: T_0 = 200 K, A_T = 200, n_0 = 5 x 10^4 /cm^3, and $\kappa_0 = 100/L$, where L is the initial width of cloud in the x direction. Typical values for L are 0.25 parsecs (pc) or 0.5 pc, where one parsec is 3.086 x 10^{18} cm. The equation state is ideal gas with adiabatic exponent $\gamma = 5/3$. With this very simple set of physics, RT models with thin initial clouds were able to reproduce the observed column density and projected velocity, as shown in Fig. [FIGKaneRT] and morphology (not shown). Cometary models appeared unsuccessful (not shown). However, recombination was omitted in these models, and there is significant evidence [{Kahn}, {Axford}, {Williams2001}] that recombination strongly suppresses RT growth. This suppression occurs because considerable absorption does in fact occur in the ablated material. As explained by Kahn and Axford [{Kahn}, {Axford}], suppression in the linear stages occurs as ablated material collects above concavities in the cloud surface and is depleted above convexities; due to recombination this effect tends to decrease ablation pressure above concavities and increase it above convexities, stabilizing the surface shape.

The second set of modeling efforts [{Mizuta2005}, {Mizuta2006}] included recombination; the work concentrated mainly on the linear regime, with some attention to the nonlinear stages and attempts to reproduce data. The code used featured two-dimensional planar Cartesian geometry. Further descriptions of the code used in these efforts are in [{Mizuta2005}, {Mizuta2006}]. The essential modifications in this newer modeling are described in those references and are summarized as follows. Recombination and associated cooling is added. Radiation is modeled as ultraviolet photons having a given energy W above the ionization energy (13.6 eV) for hydrogen. The equation of state is generalized to account for ionization and recombination. Finally, molecular cooling is added. Absorption of photons is modeled as $J_x = -a\ n\ (1-f)\ J$, where J is the photon flux, a = 6 x 10^{18} cm^2 is the cross section for photoionization, and $0 \leq f = (1-n_H/n) \leq 1$ is the ionization fraction. Accordingly, the change in f due to absorption is $\Delta f = a\ n\ (1-f)\ J\ \Delta t$, and the change in internal energy is $Wn\ a(1-f)J\ \Delta t$. Recombination is modeled as $\Delta f = -\alpha_B (n f)^2$,where α_B = 2.6 x 10^{-13} cm^3 s^{-1} is the case B recombination coefficient, with associated change in internal energy $-\beta_B k (n f)^2 T$, where $\beta_B = 1.25\ \alpha_B$ and k is Boltzmann's constant. The thermal pressure now accounts for the state of ionization, and ignores the presence of molecular hydrogen: $p_T = 2(3f+1)/(7f+5)\ \rho\ u$. To address an issue of total pressure balance between the ablated outflow and the cold cloud, a 'static, turbulent' magnetic field pressure [{Ryutov2004}] is present in the cold molecular cloud. Magnetic fields may still allow essentially compressible hydrodynamic behavior [{Ryutov2004}, {Ostriker}]. The magnetic pressure is $p_M\ (\rho/\rho_M)^{\gamma M}$, where $\gamma_M = 4/3$, and p_M and ρ_M are constants. A typical value for p_M is p_0, where $p_0 = n_{H0}\ k\ T_0$ is the initial thermal pressure, and $\rho_M = n_H\ m_H$ is the initial cloud density. The initial temperature of the cloud is assumed to be T_0 = 40 K. The results of these models [{Mizuta2005, Mizuta2006}] were that recombination strongly suppresses RT growth in the linear regime, and that by using very nonlinear initial 'perturbations', small pillar-like structures are eventually produced, possibly seeded by a separation of the ablation front from the cloud surface and probably involving nonlinear shadowing and confinement by ablation pressure.

In the most recent modeling efforts, presented here, we return to the task of reproducing quantitative observations of the Pillars. Extended details of the current model and the results will be presented elsewhere [{Kane2006}.] We use the same cylindrical code described earlier, now using the more sophisticated physics described above, and with the form of the turbulent magnetic field altered (described below). Also, the energy deposition and the structure of the initial clouds are modified, with two goals in mind. First, we want to remedy an unnatural aspect of the energy sources used previously — its artificial constancy at a boundary that is either fixed in space or translating at constant velocity (to allow the grid to follow an accelerating cloud.) Particularly when recombination is modeled, the flux at the boundary may be significantly modified by the time-dependent outflow at the boundary. Furthermore, the distance to the illuminating stars will change if the cloud accelerates, as it does in the RT models, making a constant boundary flux less realistic. Second, we want to investigate whether the RT model is aided by allowing outflow to diverge near the cloud; potentially this could thin the absorbing material between the cloud and the source, mitigating the effect of recombination. With these goals in mind, in the new modeling we use a large *r*-*z* cylindrical volume — 8 pc in the *z* direction by 4 or more pc in diameter (a large enough size was investigated that further increases in size did not change the results noticeably), which encloses the illuminating source and allows outflow to develop self-consistently. Because the initial clouds in the cometary models feature very dense central cores, the turbulent magnetic pressure $p_M (\rho/\rho_M)^{\gamma M}$ would be very large in the cores, and even at moderate density make it impossible to maintain pressure equilibrium within the cloud, at a thermal pressure corresponding to $T_0 = 40$ K. Therefore, the quantity p_M is made a spatially varying quantity $p_M(r,z)$, and is advected using the same scheme used for the other advected quantities. We set p_M inversely proportional to ρ in the initial cloud, allowing pressure equilibrium with thermal and magnetic components each initially spatially constant.

Zone widths are small near the initial cloud and in the volume which will contain the evolving and translating dense structure: $\Delta r = \Delta = 2.5 \times 10^{-3}$ pc, as in [{Mizuta2005},{Mizuta2006}]; the zone widths are larger towards the boundaries. The grid is stationary in these models. The illuminating source is a stationary single point on the *z* axis ~1.5–2 pc from the initial cloud surface; although there are several sources near the Pillars, most of the radiation comes from the nearest and brightest star [{Pound1998}.] The tips of the observed Pillars are now ~2 pc from the brightest and nearest star; we set the initial distance to the source by accounting for expected movement of the cloud. As in modeling by Richfield, Yorke and Kaisig [{RichfieldYorke}] rays are now traced obliquely across zones; this adds complexity to the task of attenuating rays and advancing *f* in time, because a zone is usually crossed by multiple rays. The initial RT cloud has finite extent in the *r* direction. The Eagle Nebula currently appears to have no lateral extent on the plane of the sky beyond the rightmost and leftmost Pillars, so it certainly appears that the transverse extent of the initial cloud was limited. This condition could aid RT, because it may further permit outflow to diverge laterally. The star luminosity is 1.2×10^{50} s^{-1}, [{Pound}]. We use the 'on-the-spot' approximation [{Cantó},{Williams2001},{Mizuta2005}], ignoring diffuse re-radiation.

We use two types of initial conditions, RT and cometary. In both the RT and cometary models, the initial gas outside the cloud has density $n_H = 10$ cm^{-3}. For the RT

simulations, the initial cloud is the same as in Ref. [{Mizuta2005}], but with finite lateral extent. The initial cloud is 0.25 pc thick in the z direction, and 0.75 pc in radius. In the current modeling we have also tried clouds of very large radius, which does not change the amount of RT growth we see (none). Two types of perturbations were used to seed RT. Here we present a model with an initial density perturbation of the form $\rho \rightarrow \rho \{1+A \exp[-\sigma_z (z-z_0)^2] \exp(-\sigma_r r^2)\}$, where z_0 is the position of the initial cloud surface, and with $A = 0.25$, $\sigma_z = [0.06 \text{ pc}/\ln(2))]^{-2}$, and $\sigma_z = [0.03 \text{ pc}/\ln(2))]^{-2}$. We have also tried dropping the central flux for 10 kyr at the start of the acceleration phase [{Mizuta2005},{Mizuta2006}], and have also tried omitting the perturbation; the results are all similar. The source is 1.5 pc from the cloud surface, since the cloud will move.

For the cometary simulations, the initial cloud is spherical with a power law density profile in the outer cloud, a central core of constant density, and continuous density at the outer radius of the core. In general, the dense initial core appears necessary to prevent the developing pillar from translating a considerable distance from the illuminating source. In [{LeflochLazareff}], the initial clouds were of constant density, and the final structure had moved five to ten times its final length. Here we present a model with initial outer radius 0.35 pc, core radius 0.04 pc, core density $n_H = 1.5 \times 10^6$ cm^{-3}, and density at the outer radius 5×10^3 cm^{-3}, with a power law exponent 2.63. We have tried many other values of the parameters given. The initial star is 2 pc from the core, because the dense core of the cloud moves little in this model.

To analyze the results of the models and compare to observations, we do two things. First, we compare the morphology (shape and size) to observations image of Pillar II [{Hester}]. Second, for the cometary models we extract predictions of projected column density ρ_{COL} and velocity v_P from the models. To obtain the projected quantities, we do the following. We assume that column density and velocity are optically thin (no self-attentuation), and that only the recombined hydrogen contributes to the observation — we take $n_{H2}(r,z) = [1-f(r,z)] \times \rho(r,z)/m_{H2}$, where $m_{H2}$is the mass of a hydrogen molecule. We then duplicate and rotate the results for $n_{H2}(r,z)$, radial velocity $v_r(r,z)$, and axial velocity $v_z(r,z)$ into three-dimensional versions $n_{H2}(x,y,z)$, radial velocity $v_r(x,y,z)$, and axial velocity $v_z(x,y,z)$, with $r^2 = x^2+y^2$. We then assume a tilt angle θ of the Pillars, where $\theta = 0$ corresponds to no tilt (Pillars in the plane of the sky), and $\theta > 0$ means the Pillar is tilted away from us. We integrate along tilted lines of sight through the three-dimensional results as follows: $\rho_{COL}(y',z') = \int n_{H2}(x,y,z)\, ds$, where $z' = z \cos(\theta)$, and $y' = y$ is in the transverse direction. Similarly, we obtain the projected velocity as $v_P(y',z') = [1/\rho_{COL}(y',z')] \int n_{H2}(x,y,z) [v_r(x,y,z) \cos(\theta) + v_y(x,y,z) \sin(\theta)]\, ds$. Finally, we convolve the results with the instrument resolution function g [{Pound1998}]: $\rho_{COL}(z') = N^{-1} G(\rho_{COL}, 0, z')$, where $G(\eta, y, z) = \iint g(y'-y, z'-z)\eta(y', z')\, dy'\, dz'$, $N^{-1} = G(1, y, z)$, and $g(y, z) = \exp[-\sigma_g (y^2+z^2)]$, with $\sigma_g = [r_F/\ln(2)]^{-2}$, where the half-maximum radius is r_F=.0325 pc. Similarly, $v_P(z') = N^{-1} G(\rho_{COL}\ v_P, 0, z')/\rho_{COL}(z')$.

3. Results

The result of the RT model at 25 kyr and 300 kyr is shown in Fig. {FIGRT1}, by contours of $\log_{10}(n_H)$. The results are typical of all RT models we have tried. At early times ablation flow develops and expands. As evidenced by the density contours toward higher radius, a somewhat divergent outflow develops. Ray divergence means the center

is pushed harder, but the edges may see increased flux due to outflow divergence and thinning. A shock is generated, which crosses the cloud in the z direction and is then reflected from the free back surface as a rarefaction. When the rarefaction returns to the front surface, the cloud recompresses and begins to accelerate. These same, initially one-dimensional events occur without recombination, in which case RT growth begins during the acceleration phase. In the current model, by 300 kyr, the cloud surface has moved about 0.75 pc. Material towards the outer radius of the initial cloud, comprising about half the initial cloud mass, is being swept in behind the cloud and confined by the ablation pressure [{Bertoldi},{BertoldiMcKee},{LeflochLazareff}], forming an inverted cup shape. At this time the diameter of the flat remainder of the front surface is about 1 pc, similar to the plane-of-sky lateral extent of the Pillars in the Eagle Nebula. There is no clear evidence of RT growth. It appears that the cloud is evolving into a very large cometary structure. Because there is no Pillar-like structure, we omit a quantitative comparison to the data.

The result of the cometary model at 25 kyr and 300 kyr is shown in Figs. {FIGcomet2} and {FIGcomet2}. Fig. {FIGcomet1} shows false color $\log_{10}(n_{\mathrm{H}})$ at the indicated times. Figure {FIGcomet2} shows the quantitative comparison to data. In Figure {FIGcomet1}, we see the outflow clearly developed by 25 kyr, and the curved shock crossing the sphere. The shock travels much faster in the more tenuous outer cloud, wrapping around and driving material in behind the core by 75 kyr. The shock reaches the core by 50 kyr and crosses the core by 75 kyr, after which time the core and surrounding material recompress and accelerate behind the departing shock; by 250 kyr the core has moved about 0.15 pc. After 75 kyr, the material behind the core is subjected to a complex set of interacting processes. Material originally behind the core collides with material swept in by the shock. Material behind the core is confined by ablation pressure, forming a cometary tail. As the material in the tail is confined and compressed, its thermal and magnetic pressure rises, but it also experiences molecular cooling. As a result, the tail radius oscillates [{LeflochLazareff}.]

In Figure {FIGcomet2}, we analyze the data using an assumed projection angle $\theta = 20^{\circ}$ at 250 kyr (for each model the choices of final time and θ are found by trial and error). The gross morphology of the Pillar appears consistent with the observed morphology of Pillar II. The column density and projected velocity gradient are consistent with the data. For both quantities, the model values appear somewhat elevated in the tip. The column density may be somewhat low in the tail. However, the column density in the tip is still less than the column density deduced by Thompson for Pillar I [xxx Thompson], meaning the model value is not unreasonable in the tip.

The model predicts a long, low-density extension to the tail. Whether such an extension is visible in the data is an open question. Visual images of the Pillars show very long, possibly limb-darkened extensions to Pillars II and III [{Castle}]. The extension in Figure {FIGcomet1} is mainly on-axis. However, we have done many other models [{Kane2007}]. In many of the other models the extension forms a shell, consistent with the observed limb-darkened wisps. Secondly, by altering the initial conditions in the model, it is easy to make the final column density lower in the tip and higher in the tail, giving agreement with the data at both locations. However, the shock

crosses a lower mass core more quickly, so that the tip recompresses and accelerates sooner, raising its velocity.

Given the simple physics and initial conditions in the model, a very detailed further comparison and a search for better initial conditions are probably not justified. In particular, the true initial conditions almost certainly featured clumps and filaments at all scales [XXX Ref]. Pillar I appears to be very clumpy at present, the small Pillar III appears possibly to be simply a filament, and other filamentary and clumpy structure are visible in several places near the Pillars [{Pound1998},{Hester}l,{Castle}]. Such features may partly account for the spatial oscillations in observed column density, and for disagreements in the tip. In addition, the line-of-sight extension of the Pillars is somewhat uncertain, as is the extent and mass of line-of-sight matter behind and in front of the Pillars [{Pound1998}].

4. Discussion

We have also performed some preliminary analysis of the earlier simulations with recombination [{Mizuta006}]. While those models are in Cartesian geometry, since we assume they are relevant to the formation of cylindrical pillars, we treat the (x,y) coordinates as (r,z) coordinates and proceed with the analysis already described, beginning by rotating and duplicating the two-dimensional result into a three-dimensional result. With a very nonlinear initial density 'perturbation', by 400 kyr small globular structures appear and elongate by 460 kyr as the remainder of the cloud accelerates. Analyzing these results, we find that the velocity gradients near the tips are consistent with the observations. Morphologically, the structures are low mass, five to eight solar masses compared to ~100 solar masses for Pillar II, and the column density drops off sharply about 0.2–0.3 pc from the tip. A possible formation mechanism for these structures is discussed in [{Mizuta2006}]. The evolution of the structure appears somewhat similar to that proposed for the much smaller globules in the Helix Nebula [{O'DellHandron},{Capriotti}]. Their growth is probably strongly affected by the cometary processes of shadowing and of confinement by ablation pressure. Overall, the evolved structures appear to be low-mass comets.

In the new models presented here, the contact between the diverging outflow and the surrounding medium reaches the snowplow phase and stalls inside the simulation boundaries. Whether this implies a corresponding observable feature in the vicinity of the Eagle Nebula is unclear. In all of these models, we neglect mass outflow from the illuminating stars, which could lead to observable bow shocks [XXX {Ref}]; these, however, have not been observed near M16 [XXX {Ref}].

5. Conclusions

When the essential physics of recombination is included, it appears easier to reconcile cometary models with observations of Pillar II of the Eagle Nebula than to do so with RT models. There is no growth in the RT models, whether the cloud is of infinite or finite lateral extent. Cometary models with a dense initial core appear to do well in morphology, projected column density, and projected velocity. In these models we use a simple treatment of deposition, cooling, and magnetic support pressure, and ignore diffuse re-radiation. In

contrast to the RT models, the cometary models presented here are conceptually simple — spatially symmetric, making no assumptions about initial orientation or perturbation. The dense initial core appears to be a key component of the cometary model, and in general the clumpy, filamentary nature of molecular clouds appear closely connected to Pillar formation.

This work was performed under the auspices of the U.S. Department of Energy by the University of California, Lawrence Livermore National Laboratory under Contract No. W-7405-Eng-48. MWP supported by NSF Grant No. AST-0228974.

References

{Hester}. Hester, J.J., Scowen, P.A., Sankrit, R. et al: 1996, *Astronomical Journ*. **111** 2349.
{Pound1998}. Pound, M.W.: 1998, *ApJ*, **493**, L113.
[Pound2006}. Pound, M.W. *et al*., this issue.
{Ryutov2006}. Ryutov, D.D. *et al*., this issue
{Thompson}. Rodger I. Thompson, Bradford A. Smith, and J. Jeff Hester 2002 ApJ, 570, 749
{Spitzer}. Spitzer, ApJ **120**, 1 (1954)
{Frieman}. Frieman, ApJ **120**, 18 (1954)
{Williams2001}. Williams, Ward-Thompson & Whitworth, Mon. Not R. Astron. Soc. **327**, 788 (2001)
{Cantó}. Cantó, J., Raga A.C., Steffen W., Shapiro P.R., ApJ, 502,695 (1998)
{Osterbrock}. Osterbrock, ApJ **125**, 6220 (1957)
{O'DellHandron}. O'Dell, C. R. & Handron, K., AJ 111, 130 (1996)
{Capriotti}. Capriotti, ApJ **179**, 495 (1973
{RichlingYorke2000}. Richling & Yorke ApJ **539**, 258 (2000)
{RichlingYorke2000}. Richling & Yorke ,A&A **327**, 317 (1997)
{YorkeKaisig}. Yorke & Kaisig, Comp. Phys. Comm., 89, 29 (1995)
{Kahn}. Kahn, Rev. Mod. Phys. **30**, 1058 (1958)
{Vandervoort}. Vandervoort, ApJ **135,** 212 (1962)
{Axford}. Axford, ApJ **140,** 112 (1964)
{Reipurth}. Reipurth, A&A **117** (1983)
{Bertoldi }. Bertoldi, ApJ **346**, 735 (1989)
{BertoldiMcKee }. Bertoldi & McKee, ApJ **354**, 529 (1990)
{Williams2002}. Williams, Mon. Not R. Astron. Soc. **331**, 693 (2002)
{LeflochLazareff }. Lefloch & Lazareff, A&A **289**, 559 (1994); A&A **301**, 522 (1995)
{Neufeld}. D.A. Neufeld and M.J. Kaufman, ApJ, **418**, 263 (1993); Neufeld *et al*., ApJS **100,** 132 (1995)
{Ostriker}. Ostriker, Gammie, & Stone, ApJ **513,** 259 (1999); ApJ **546,** 980 (2001).
{Kane2001} Kane, H. F. Robey, B. A. Remington *et. al*, Physical Review E Rapid Communications 055401(R) (April, 2001).
{Kane2006} In preparation.
{Ryutov2004} Ryutov et al., Proc. 5th Conf. HEDLA, AIP **703**, 415 (2004).
{Mizuta2005}. Mizuta *et al*.,ApJ **621**, 803–807, (2005)
{Mizuta2006}. Mizuta *et al*., this issue.

{Castle}. Harvard Smithsonian Center for Astrophysics 'Castle' image of Eagle Nebula taken at Whipple Observatory by Peter Challis: http://cfa-www.harvard.edu/cfa/hotimage/m16.html (no publication found.)
{ZEUS}. Stone, J. M., Norman, M. L., The Astrophysical Journal Supplement Series **80**, 753 (1992)
{vanLeer}. van Leer, B. J. Comput. Phys. **23**, 276 (1977).
{Sysoev}. Sysoev N. E., Astron. Lett. **23**, 409 (1997)

Figure captions

Fig. {FIGKaneRT}
Early modeling of Pillar II without recombination. Left panel: model projected velocity (red) versus data (solid squares). Dashed lines are a simple incompressible RT model [{Pound},{Frieman},{Spitzer}]. Right panel: model column density (red) versus data (black).

Figure {FIGRT1}
Current RT model with recombination and finite-radius initial cloud at 25 kyr. Simulated $\log_{10}(n_H\ cm^3)$ contours: 3, 3.5, 4, 5.

Figure {FIGRT2}
Current RT model with recombination and finite-radius initial cloud at 75 kyr.

Figure {FIGcomet1}
False color $\log_{10}(n_H\ cm^3)$ contours in current cometary model with recombination.

Figure {FIGcomet2}
Quantitative comparion of current cometary model with recombination to observation. Center: Projected model $\log_{10}(n_H\ cm^3)$ contours (3, 3.5, 4, 5) overlaid on image of Pillar II [{Hester}]. Top: column density versus projected position. Bottom: projected velocity versus projected position.

Fig. {FIGKaneRT}

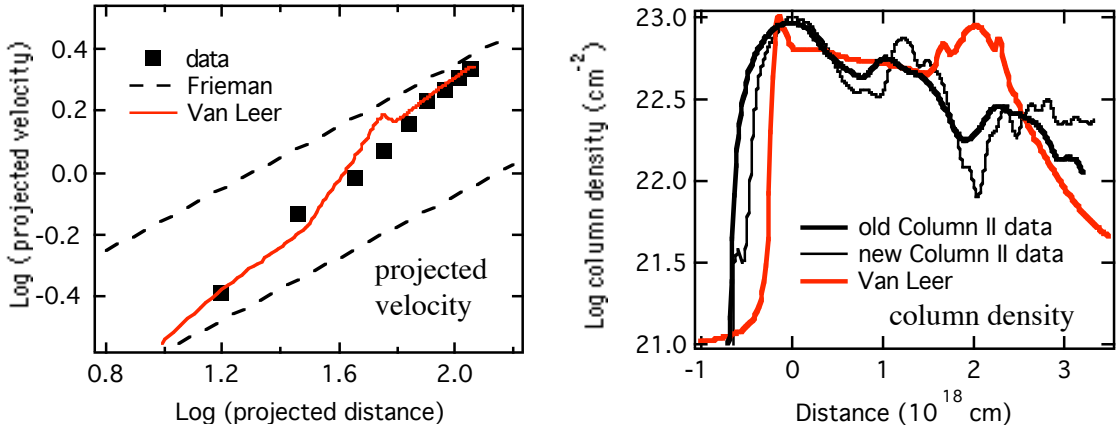

Fig. {FIGRT1}

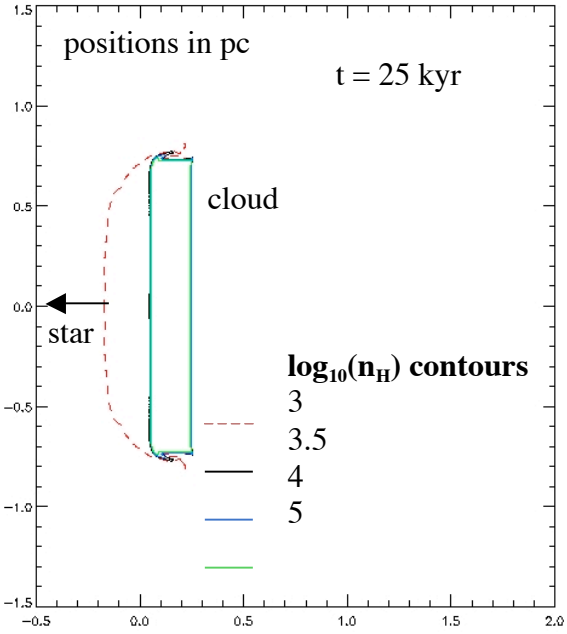

Fig. {FIGRT2}

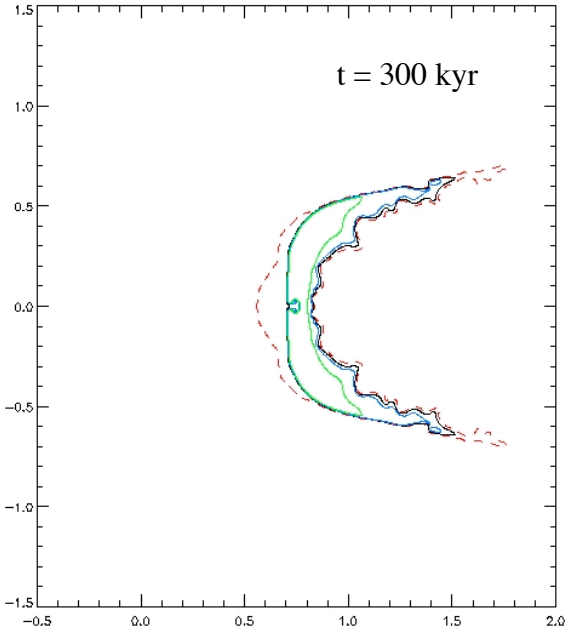

Fig. {FIGcomet1}

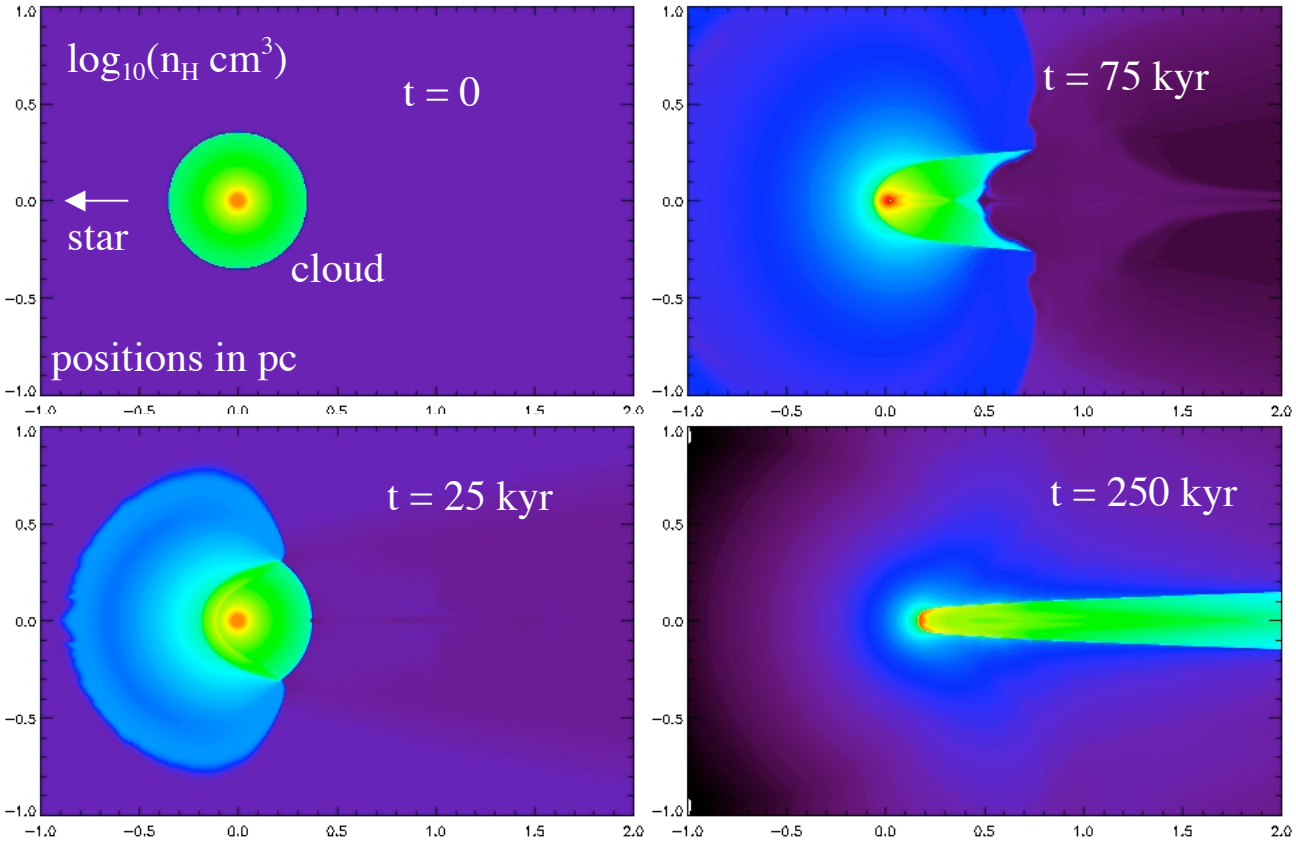

Fig. {FIGcomet2}